DALAT UNIVERSITY JOURNAL OF SCIENCE Volume 13, Issue 1, 2023 45-58

STUDY OF NEGATIVE REFRACTIVE INDEX IN Rb FOUR-LEVEL N-TYPE ATOMIC GAS MEDIUM

Nguyen Huy Bang[a], Le Nguyen Mai Anh[b], Le Thi Minh Phuong[c], Ho Hai Quang[a], Le Van Doai[a*]

[a]*Vinh University, Nghe An, Vietnam*
[b]*The Faculty of Science, Nong Lam University, Ho Chi Minh City, Vietnam*
[c]*Saigon University, Ho Chi Minh City, Vietnam*
[*]*Corresponding author: Email: doailv@vinhuni.edu.vn*

Article history
Received: February 9th, 2022
Received in revised form: March 12th, 2022 | Accepted: March 28th, 2022
Available online: October 4th, 2022

Abstract

In this work, we study the generation of a negative refractive index based on electromagnetically induced transparency (EIT) in a Rb four-level N-type atomic gas medium. We derive analytic expressions for the relative permittivity and relative permeability of the medium according to the parameters of the probe, pump, and signal laser fields. We then investigate the variation of the real parts of the relative permittivity and relative permeability with respect to the intensity and frequency of the pump and signal laser fields. In the presence of the pump laser beam, the medium becomes transparent to the probe laser beam even in the resonant region. At the same time, the real parts of the relative permittivity and relative permeability are simultaneously negative (i.e., the medium exhibits a negative refractive index) in the EIT spectral domain. In the presence of the signal laser beam, the EIT effect occurs over two different frequency domains of the probe beam, so a negative refractive index is also generated in these two frequency domains. The investigation of the real parts of the relative permittivity and relative permeability with intensity and frequency of the pump and signal laser fields allowed us to find the laser parameters for the appearance of the negative refractive index, which can be useful for experimental observations.

Keywords: Electromagnetically induced transparency; Four-level N-type atomic system; Negative refractive index.

DOI: https://doi.org/10.37569/DalatUniversity.13.1.1028(2023)

Article type: (peer-reviewed) Full-length research article

Copyright © 2022 The author(s).

Licensing: This article is published under a CC BY-NC 4.0 license.

1. INTRODUCTION

The propagation of electromagnetic waves in a medium is characterized by the relative permittivity ε_r and relative permeability μ_r of the medium; that is, it depends on the refractive index of the material $n^2 = \varepsilon_r\mu_r$. The refractive index is a complex quantity, but usually only the positive refractive index is used, i.e., both the relative permittivity and relative permeability are simultaneously positive ($n = \sqrt{\varepsilon_r\mu_r} > 0$). However, Veselago (1968) proposed a theory of materials with negative refractive index, i.e., both the relative permittivity and relative permeability are simultaneously negative at a definite frequency. These are called left-handed materials or negative index materials. This type of material has opened up a new research area in material technology and has many practical applications, such as reversals of Doppler shift and Cherenkov radiation (Veselago, 1968), amplification of evanescent waves (Pendry, 2000), subwavelength focusing (Aydin et al., 2007), negative Goos-Hänchen shift (Berman, 2002), perfect lens (Williams, 2001), etc.

Currently, there are several methods to create negative refractive index materials, including artificial composite metamaterials (Pendry, 2003), photonic crystal structures (Cubukcu et al., 2003), chiral materials (Yannopapas, 2006), etc. In these artificial left-handed materials, the achieved negative refractive index is often accompanied by strong absorption, especially in the resonant frequency domain. Therefore, the study and fabrication of negative refractive index materials in the optical frequency domain without absorption are of great significance.

In the past few decades, the discovery of electromagnetically induced transparency (EIT) has provided a breakthrough method to reduce or even completely eliminate resonance absorption (Boller et al., 1991). EIT is a quantum interference phenomenon that occurs between probability amplitudes within an atomic system when excited by laser fields. This interference can lead to either an enhancement (constructive interference) or a complete cancellation (destructive interference) in the total transition probability. The consequence of this interference can lead to a profound change in linear and nonlinear optical properties of a medium (Nguyen et al., 2019). The basic configurations for the EIT effect are three-level atomic systems consisting of lambda, ladder, and V-type configurations. However, in three-level atomic systems, we can only create one narrow wavelength domain at which light becomes transparent (called the EIT window) (Nguyen et al., 2019). Therefore, the extension of the transparent spectral domain is of great interest to research groups. This can be done in four-, five-, and even six-level atomic systems. Indeed, McGloin et al. (2001) investigated an atomic system consisting of N-levels excited by (N−1) laser fields to produce (N−2) EIT windows. To date, many applications of the EIT effect have been reported, such as lasing without inversion (Le & Vo, 2020), giant Kerr nonlinearity (Le & Dinh, 2021), slow light (Nguyễn et al., 2017), low threshold optical bistability (Phan et al., 2016), optical soliton (Dong et al., 2016), all-optical switching (Jafarzadeh, 2017), etc.

The discovery of the EIT effect opens up a simple way to achieve a negative refractive index for an atomic gas medium in the optical domain with a very significant reduction in absorption. At the same time, the negative refractive index range is easily changed toward short or long wavelengths. Indeed, Oktel and Müstecaplıoğlu (2004) and Shen et al. (2004) first proposed a scheme for realization of the negative refractive index in a three-level lambda-type atomic medium under the EIT condition. Later, Liu et al. (2009) showed that left-handed properties can be electromagnetically induced in a Λ-type four-level scheme in Er^{3+}:$YAlO_3$ crystal. Zhang et al. (2008) obtained a negative refractive index in a four-level atomic medium and showed that it is possible to switch between positive and negative refractive indices by changing the relative phase of the applied fields. Recently, Krowne and Shen (2009) realized a negative refractive index using dressed-state mixed parity transitions of atoms, and Dutta and Dastidar (2010) used interference of spontaneous emissions to obtain a negative refractive index in a three-level lambda atomic configuration. Negative refractive indices have also been reported in four-level V-type (Zhang et al., 2007), four-level Y-type (Zhao et al., 2010), four-level Ξ+V (Zhao et al., 2013), and four-level cascade (Fang et al., 2016) atomic systems as well as in a five-level atomic system (Othman & Yevick, 2016). In addition to the atomic medium, a negative refractive index was also obtained in a molecular medium under EIT conditions (Sardar et al., 2021). More recently, the influence of Doppler broadening on the negative refractive index in three-level lambda (Nguyen et al., 2022) and four-level inverted Y configurations (Nguyen et al., 2021) has also been considered.

In this work, we study the negative refractive index in a four-level N-type atomic system based on electromagnetically induced transparency. By solving the density matrix equations, we derive the expressions of relative permittivity and relative permeability according to the laser parameters. The influence of the laser parameters on the negative refractive index are investigated.

2. THEORETICAL MODEL

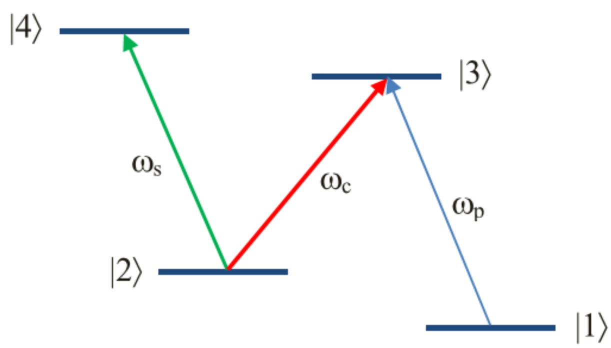

Figure 1. The four-level N-type atomic configuration excited by the probe, pump, and signal laser fields

We consider an N-level four-level atomic configuration interacting with three laser fields, as depicted in Figure 1. In which, the transitions $|1\rangle \leftrightarrow |3\rangle$, $|2\rangle \leftrightarrow |3\rangle$, and $|2\rangle \leftrightarrow |4\rangle$ are electric dipole allowed, while the transition $|1\rangle \leftrightarrow |2\rangle$ is magnetic dipole allowed. Therefore, the electric field of the probe laser beam can excite the transition $|1\rangle \leftrightarrow |3\rangle$, while the magnetic field of the probe beam induces the transition $|1\rangle \leftrightarrow |2\rangle$. The transition $|2\rangle \leftrightarrow |3\rangle$ is excited by the pump laser beam, and the transition $|2\rangle \leftrightarrow |4\rangle$ is excited by the signal laser beam. We denote ω_p, ω_c, and ω_s as the angular frequencies of the probe, pump, and signal laser beams, respectively.

The evolution of the quantum states of the atomic system in the laser fields is represented by the Liouville density matrix equation, as follows (Nguyen et al., 2019):

$$\dot{\rho} = -\frac{i}{\hbar}[H, \rho] + \Lambda\rho \tag{1}$$

where $H = H_0 + H_I$ is the total Hamiltonian, H_0 is the Hamiltonian of the free atom, H_I is the interaction Hamiltonian, and $\Lambda\rho$ represents decay processes in the atomic system. We have

$$H_0 = \sum_{i=1}^{4} \hbar\omega_i |i\rangle\langle i| \tag{2}$$

$$H_I = -\frac{\hbar\Omega_p}{2}\left(|1\rangle\langle 3| e^{i\omega_p t} + c.c.\right) - \frac{\hbar\Omega_c}{2}\left(|2\rangle\langle 3| e^{i\omega_c t} + c.c.\right) - \frac{\hbar\Omega_s}{2}\left(|2\rangle\langle 4| e^{i\omega_s t} + c.c.\right) \tag{3}$$

where *c.c.* describes the complex conjugate term. From Equations (1) – (3), we have derived a set of density matrix equations for the population and atomic coherence, as follows:

$$\dot{\rho}_{11} = \Gamma_{21}\rho_{22} + \Gamma_{31}\rho_{33} + \Gamma_{41}\rho_{44} + \frac{i}{2}\Omega_p(\rho_{31} - \rho_{13}) \tag{4}$$

$$\dot{\rho}_{22} = \Gamma_{42}\rho_{44} + \Gamma_{32}\rho_{33} - \Gamma_{21}\rho_{22} + \frac{i}{2}\Omega_c(\rho_{32} - \rho_{23}) + \frac{i}{2}\Omega_s(\rho_{42} - \rho_{24}) \tag{5}$$

$$\dot{\rho}_{33} = \Gamma_{43}\rho_{44} - \Gamma_{32}\rho_{33} - \Gamma_{31}\rho_{33} + \frac{i}{2}\Omega_s(\rho_{23} - \rho_{32}) + \frac{i}{2}\Omega_p(\rho_{13} - \rho_{31}) \tag{6}$$

$$\dot{\rho}_{44} = -\left(\Gamma_{43} + \Gamma_{42} + \Gamma_{41}\right)\rho_{44} + \frac{i}{2}\Omega_s(\rho_{24} - \rho_{42}) \tag{7}$$

$$\dot{\rho}_{21} = -\left[i(\Delta_p - \Delta_c) + \gamma_{21}\right]\rho_{21} + \frac{i\Omega_c}{2}\rho_{31} - \frac{i\Omega_p}{2}\rho_{23} + \frac{i\Omega_s}{2}\rho_{41} \tag{8}$$

$$\dot{\rho}_{31} = -\left(i\Delta_p + \gamma_{31}\right)\rho_{31} + \frac{i\Omega_p}{2}(\rho_{11} - \rho_{33}) + \frac{i\Omega_c}{2}\rho_{21} \tag{9}$$

$$\dot{\rho}_{41} = -\left[i(\Delta_p - \Delta_c + \Delta_s) + \gamma_{41}\right]\rho_{41} + \frac{i\Omega_s}{2}\rho_{21} - \frac{i\Omega_p}{2}\rho_{43} \tag{10}$$

$$\dot{\rho}_{32} = -\left(i\Delta_c + \gamma_{32}\right)\rho_{32} + \frac{i\Omega_c}{2}(\rho_{22} - \rho_{33}) + \frac{i\Omega_p}{2}\rho_{12} - \frac{i\Omega_s}{2}\rho_{34} \tag{11}$$

$$\dot{\rho}_{42} = \left[i\Delta_s - \gamma_{42}\right]\rho_{42} + \frac{i\Omega_s}{2}(\rho_{22} - \rho_{44}) - \frac{i\Omega_c}{2}\rho_{43} \tag{12}$$

$$\dot{\rho}_{43} = -\left[i(\Delta_s - \Delta_c) + \gamma_{43}\right]\rho_{43} + \frac{i\Omega_s}{2}\rho_{23} - \frac{i\Omega_p}{2}\rho_{41} - \frac{i\Omega_c}{2}\rho_{42} \tag{13}$$

where $\Delta_p = \omega_p - \omega_{31}$, $\Delta_c = \omega_c - \omega_{32}$, and $\Delta_s = \omega_s - \omega_{42}$ are the frequency detunings of the probe, pump, and signal fields, respectively; $\Omega_p = d_{31}E_p/\hbar$, $\Omega_c = d_{32}E_c/\hbar$, and $\Omega_s = d_{42}E_s/\hbar$ are the Rabi frequencies of the probe, pump, and signal fields, respectively; and d_{ik} is the electric-dipole matrix element. We denote γ_{ij} as the decay rate of the atomic coherences ρ_{ik} and Γ_{ik} as the decay rate of the population from the $|i\rangle$ level to the $|k\rangle$ level.

Now, we solve the set of density matrix Equations (4) – (13) in the steady-state condition ($\partial\rho/\partial t = 0$) to find the solutions for ρ_{31} and ρ_{21}, which are related to the electric and magnetic responses of the medium for the probe light. Under the condition that the probe laser field is much weaker than the pump and signal laser fields, we obtain from Equation (10)

$$\rho_{41} = \frac{i\Omega_s}{2\left[i(\Delta_p - \Delta_c + \Delta_s) + \gamma_{41}\right]}\rho_{21}. \tag{14}$$

Substituting (14) into Equation (8), we have

$$\rho_{21} = \frac{i\Omega_c}{2}\frac{\rho_{31}}{i(\Delta_p - \Delta_c) + \gamma_{21} + \dfrac{\Omega_s^2/4}{i(\Delta_p - \Delta_c + \Delta_s) + \gamma_{41}}} \equiv \frac{i\Omega_c}{2}\frac{\rho_{31}}{A} \tag{15}$$

with $A = i(\Delta_p - \Delta_c) + \gamma_{21} + \dfrac{\Omega_s^2/4}{i(\Delta_p - \Delta_c + \Delta_s) + \gamma_{41}}$.

By substituting (15) into Equation (9) we find the solution of ρ_{31} as follows:

$$\rho_{31} = \frac{i\Omega_p/2}{i\Delta_p + \gamma_{31} + \dfrac{\Omega_c^2/4}{i(\Delta_p - \Delta_c) + \gamma_{21} + \dfrac{\Omega_s^2/4}{i(\Delta_p - \Delta_c + \Delta_s) + \gamma_{41}}}} \equiv \frac{i\Omega_p/2}{B} \tag{16}$$

with $B = i\Delta_p + \gamma_{31} + \dfrac{\Omega_c^2/4}{i(\Delta_p - \Delta_c) + \gamma_{21} + \dfrac{\Omega_s^2/4}{i(\Delta_p - \Delta_c + \Delta_s) + \gamma_{41}}} \equiv i\Delta_p + \gamma_{31} + \dfrac{\Omega_c^2/4}{A}$.

The solution of ρ_{21} can be found by substituting (16) into (15) as follows:

$$\rho_{21} = \frac{-\Omega_c \Omega_p}{4A.B}. \tag{17}$$

According to classical electrodynamic theory, for an atomic gas medium, the electric susceptibility (χ_e) and magnetic susceptibility (χ_m) are related to the density matrix elements, ρ_{31} and ρ_{21}, by the following relations (Shen et al., 2004):

$$\chi_e = \frac{2Nd_{31}\rho_{31}}{\varepsilon_0 E_p} \tag{18}$$

$$\chi_m = \frac{2Nm_{21}\rho_{21}}{H_p} \tag{19}$$

where N denotes the atomic density, d_{21} and m_{31} are respectively the electric and magnetic dipole matrix elements, and E_p and H_p denote the electric and magnetic field envelopes of the probe field.

On the other hand, the relative permittivity ε_r and relative permeability μ_r of the medium are related to the electric and magnetic susceptibilities according to the following relationships:

$$\varepsilon_r = 1 + \chi_e \tag{20}$$

$$\mu_r = 1 + \chi_m \tag{21}$$

Substituting expression (16) into (18) we get the expression of electric susceptibility as

$$\chi_e = \frac{iNd_{31}^2}{\varepsilon_0 \hbar}\frac{1}{B}. \tag{22}$$

To find the expression of the magnetic susceptibility χ_m, we use the relationship between the electric and magnetic fields of the light field, as follows:

$$H_p = \sqrt{\varepsilon_r \varepsilon_o / \mu_r \mu_o} E_p \tag{23}$$

where ε_0 is the dielectric constant and μ_0 is the permeability of vacuum. Therefore, expression (19) can be written in the following form:

$$\chi_m = \frac{2Nm_{21}\rho_{21}}{\sqrt{\varepsilon_r\varepsilon_0 / \mu_r\mu_0}E_p} \tag{24}$$

$$\chi_m = \frac{2Nm_{21}}{E_p}\sqrt{\frac{\mu_r\mu_0}{\varepsilon_r\varepsilon_0}}\rho_{21} = \frac{2Nm_{21}}{\varepsilon_0 E_p}\sqrt{\frac{(1+\chi_m)\varepsilon_0\mu_0}{(1+\chi_e)}}\rho_{31} \tag{25}$$

$$\chi_m = \frac{2Nm_{21}}{c\varepsilon_0 E_p}\sqrt{\frac{(1+\chi_m)}{(1+\chi_e)}}\rho_{21}. \tag{26}$$

Here, we have substituted $c = 1/\sqrt{\varepsilon_0\mu_0}$, which is the speed of light in a vacuum.

Substituting expression (15) into (26), we obtain

$$\chi_m = \left(\frac{im_{21}}{2cd_{31}}\frac{\Omega_c}{A}\right)\sqrt{\frac{(1+\chi_m)}{(1+\chi_e)}}\chi_e. \tag{27}$$

In the derivation of expression (27), we used $\rho_{31} = \frac{\varepsilon_0 E_p \chi_e}{2Nd_{31}}$, which is derived from Equation (18). Squaring both sides of Equation (27), we have

$$\chi_m^2 = -\left(\frac{m_{21}}{2cd_{31}}\frac{\Omega_c}{A}\right)^2 \frac{(1+\chi_m)}{(1+\chi_e)}\chi_e^2 \tag{28}$$

$$\chi_m^2 + \frac{\chi_e^2}{1+\chi_e}\left(\frac{m_{21}}{2cd_{31}}\frac{\Omega_c}{A}\right)^2 \chi_m + \frac{\chi_e^2}{1+\chi_e}\left(\frac{m_{21}}{2cd_{31}}\frac{\Omega_c}{A}\right)^2 = 0 \tag{29}$$

We set

$$F = \frac{\chi_e}{\sqrt{1+\chi_e}}\left(\frac{m_{21}}{2cd_{31}}\frac{\Omega_c}{A}\right). \tag{30}$$

Therefore, Equation (29) is rewritten as

$$\chi_m^2 + F^2\chi_m + F^2 = 0. \tag{31}$$

Equation (29) has the following solutions:

$$\chi_m^{\pm} = \frac{-F^2 \pm \sqrt{F^4 - 4F^2}}{2}. \tag{32}$$

Thus, the relative permeability has the corresponding solutions:

$$\mu_r^{\pm} = 1 + \frac{-F^2 \pm \sqrt{F^4 - 4F^2}}{2}. \tag{33}$$

We note that, to ensure the relative permeability can be negative, the negative root μ_r^- in Equation (33) will be used for the following investigations.

With the expressions for relative permittivity ε_r and relative permeability μ_r, the refractive index of the left-handed medium can be determined by (Veselago, 1968)

$$n = -\sqrt{\varepsilon_r \mu_r}\ . \tag{34}$$

3. RESULTS AND DISCUSSION

We apply the analytical model to the ^{87}Rb atom, where $|1\rangle$ and $|2\rangle$ are two hyperfine levels of the ground state, $|1\rangle = |5S_{1/2}, F = 1\rangle$ and $|2\rangle = |5S_{1/2}, F = 2\rangle$, and $|3\rangle$ and $|4\rangle$ are two hyperfine levels of the excited state, $|3\rangle = |5P_{3/2}, F' = 2\rangle$ and $|4\rangle = |5P_{3/2}, F' = 3\rangle$. The atomic parameters (Steck, 2019) are $N = 3.5\times10^{23}$ atoms/m^3, $\Gamma_{42} = \Gamma_{32} = \Gamma_{31} = 6$ MHz, $d_{31} = 1.6\times10^{-29}$ C·m, $m_{21} = 7.26\times10^{-23}$ A·m^2, and $\omega_p = 3.77\times10^8$ MHz.

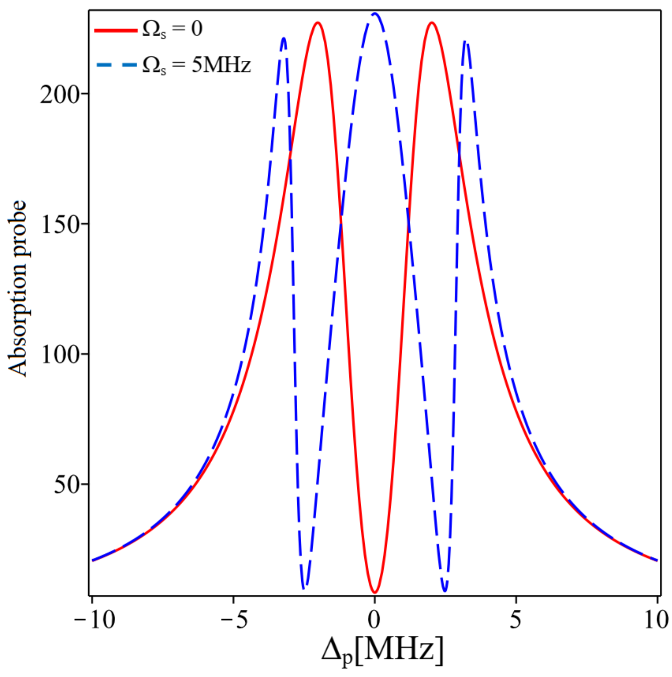

Figure 2. Simulation of the EIT spectrum of the probe laser beam in the absence (solid line) and presence (dashed line) of the signal laser beam

Note: The parameters of the pump laser are $\Delta_c = 0$ and $\Omega_c = 4$ MHz, while the parameters of the signal laser are $\Delta_s = 0$, $\Omega_s = 0$ (solid line) and $\Omega_s = 5$ MHz (dashed line).

With the arrangement of laser beams that excite atomic transitions in a four-level N-type configuration, as shown in Figure 1, the pump laser beam (Ω_c) can induce the EIT effect for the probe beam (Ω_p), while the signal laser beam can alter the EIT effect. To see this, in Figure 2 we plot the absorption coefficient of the probe beam Im(ε_r) in the absence (solid line) and the presence (dashed line) of the signal laser beam (Ω_s). The parameters of the pump laser beam are chosen as Ω_c = 4 MHz and Δ_c = 0.

From the solid line in Figure 2, we see that in the absence of the signal laser beam (i.e., intensity or Rabi frequency Ω_s = 0), a transparent spectral region appears on the absorption profile of the probe beam (i.e., the absorption coefficient is completely suppressed) at the resonant frequency Δ_p = 0. This phenomenon is known as electromagnetically induced transparency, and the transparent spectral region is called the EIT window (Nguyen et al., 2019). This EIT effect is produced by the induction of the pump laser beam. For a deeper understanding of the EIT effect, readers can see the reference (Nguyen et al., 2019).

In the presence of a signal laser beam with intensity Ω_s = 5 MHz (see dashed line in Figure 2), we see two EIT windows appear on the absorption profile of the probe beam. These two EIT windows are symmetric around the atomic resonance frequency Δ_p = 0. This leads to the resonance domain becoming the maximum absorption domain.

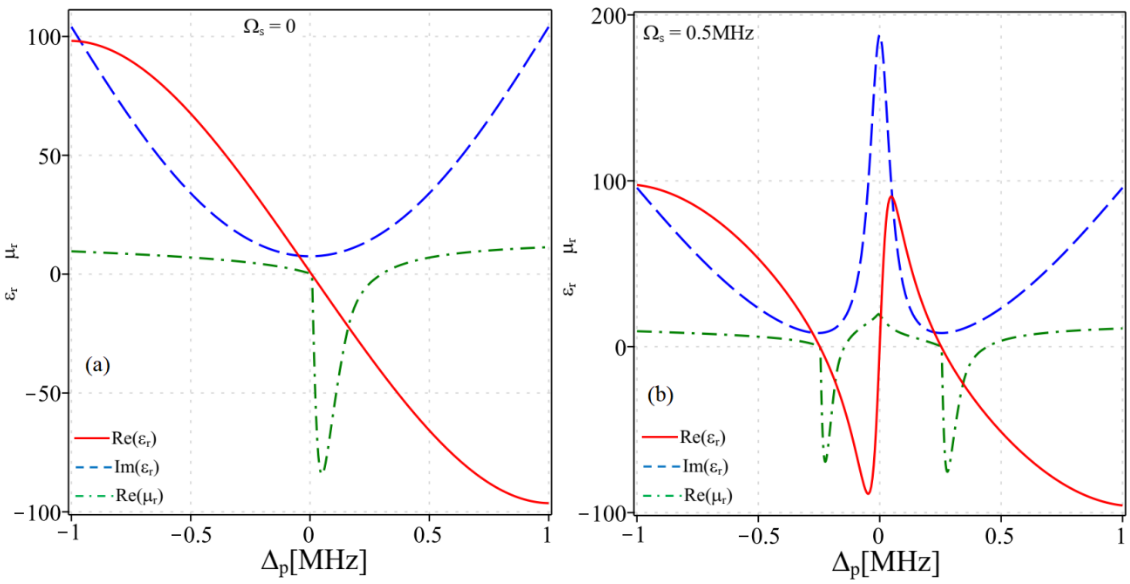

Figure 3. Plots of Re(ε_r) (solid line) and Re(μ_r) (dash-dotted line) versus probe frequency detuning Δ_p in the absence (a) and presence (b) of the signal laser beam

Note: The parameters of the pump laser are Δ_c = 0 and Ω_c = 4 MHz, while the parameters of the signal laser are Δ_s = 0, Ω_s = 0 (a) and Ω_s = 0.5 MHz (b). The dashed line is the absorption of the probe laser beam Im(ε_r).

The occurrence of EIT windows is the basis for achieving a negative refractive index with simultaneously negative permittivity and permeability. Indeed, as in Figure 3, we plot Re(ε_r) and Re(μ_r) in the absence (a) and the presence (b) of the signal laser beam with the pump laser parameters chosen as Ω_c = 4 MHz and Δ_p = 0. Figure 3(a) shows that the real parts of the relative permittivity Re(ε_r) and relative permeability Re(μ_r) are simultaneously negative in the probe frequency detuning range $0 < \Delta_p < 0.3$ MHz, which means that the medium exhibits a negative refractive index in the spectral domain $0 < \Delta_p < 0.3$ MHz. This spectral domain is also in the EIT spectral domain, as we see in Figure 2. On the other hand, the appearance of two EIT windows in the presence of the signal laser beam also leads to the appearance of two negative refractive index ranges, as shown in Figure 3(b). That is, the real parts of the relative permittivity Re(ε_r) and relative permeability Re(μ_r) are simultaneously negative in the two frequency detuning ranges –0.25 MHz < Δ_p < –0.15 MHz and 0.25 MHz < Δ_p < 0.35 MHz. These two negative refractive index ranges are also in the EIT spectral domains, which means that the negative refractive index is produced with very small absorption and even complete suppression. This is the outstanding advantage of negative refractive index materials using the EIT technique.

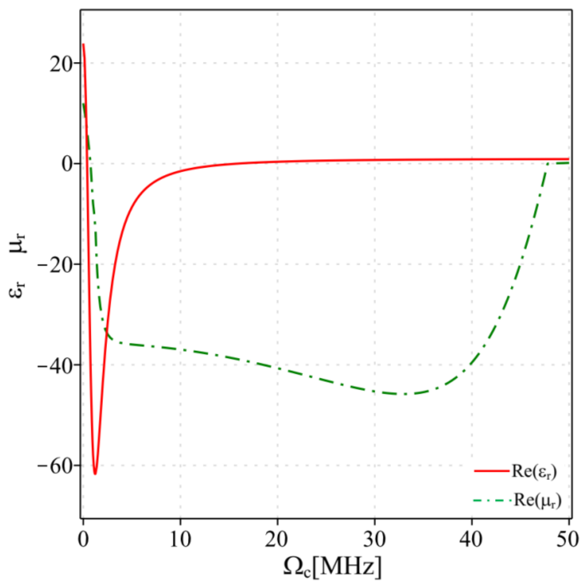

Figure 4. Variations of Re(ε_r) (solid line) and Re(μ_r) (dash-dotted line) with pump frequency Rabi Ω_c when the signal laser intensity is fixed at Ω_s = 0.5 MHz

Note: Other parameters are Δ_p = 0.3 MHz and $\Delta_s = \Delta_c = 0$.

Next, in Figure 4 we investigate the variation of the real parts of the relative permittivity Re(ε_r) and relative permeability Re(μ_r) with respect to the pump laser intensity when the signal laser intensity is fixed at Ω_s = 0.5 MHz. Here, we choose the probe laser frequency at the frequency detuning Δ_p = 0.3 MHz, which is in the negative refractive index region, as investigated in Figure 3. The investigation in Figure 4 shows that both Re(ε_r) and Re(μ_r) vary from positive to negative and vice versa as the pump laser Rabi frequency (or intensity) increases from 0 to 50 MHz. However, Re(ε_r) and

Re(μ_r) are simultaneously negative (or the medium exhibits negative refractive index) when the pump laser intensity is in the range 2 MHz < Ω_c < 10 MHz.

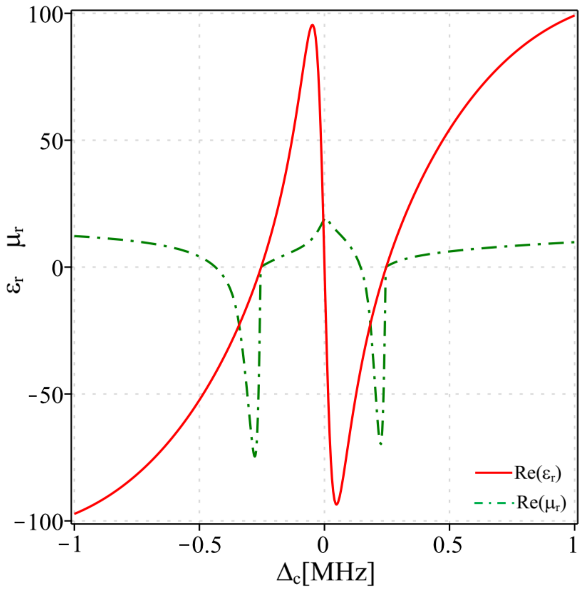

Figure 5. Variations of Re(ε_r) (solid line) and Re(μ_r) (dash-dotted line) with respect to pump frequency detuning Δ_c when other parameters are fixed at Ω_c = 4 MHz, Ω_s = 0.5 MHz, and $\Delta_p = \Delta_s = 0$

Finally, in Figure 5 we investigate the variation of the real parts of the relative permittivity Re(ε_r) and relative permeability Re(μ_r) with respect to the pump laser frequency detuning when other laser parameters are fixed at Ω_c = 4 MHz, Ω_s = 0.5 MHz, and $\Delta_p = \Delta_s = 0$. Figure 5 shows that at a specified probe frequency (with $\Delta_p = 0$), the medium has a negative refractive index (Re(ε_r) and Re(μ_r) are simultaneously negative) and the two frequency domains of the pump laser are –0.35 MHz < Δ_c < –0.25 MHz and 0.15 MHz < Δ_c < 0.25 MHz. That is, there is a similarity, as shown in Figure 3(b). This is because the EIT effect appears to satisfy the two-photon resonance condition $\Delta_p + \Delta_c$ = 0 (Nguyen et al., 2019).

4. CONCLUSION

By solving the set of density matrix equations in the weak probe field approximation, we have found expressions for the relative permittivity and relative permeability of a four-level N-type atomic medium. Thereby, we investigated the variation of the real parts of the relative permittivity and relative permeability with respect to the intensity and frequency of the pump and signal laser fields. In the presence of the pump laser beam, the medium becomes transparent to the probe laser beam even in the resonant region, and the real parts of the relative permittivity and permeability are simultaneously negative (i.e., the medium exhibits negative refractive index) in the EIT spectral domain. In the presence of the signal laser beam, the EIT effect occurs over two different frequency domains of the probe beam, so a negative refractive index is also generated in these two frequency domains. The investigation of the real parts of the relative permittivity and relative permeability with respect to the intensity and frequency of the laser fields allowed us to find the laser parameters for achieving a negative refractive index. Our analytical model can be useful for experimental observations and related applications.

ACKNOWLEDGMENTS

The financial support from the Vietnamese National Foundation for Science and Technology Development (NAFOSTED) through the grant code 103.03-2019.383 is acknowledged.

REFERENCES

Aydin, K., Bulu, I., & Ozbay, E. (2007). Subwavelength resolution with a negative-index metamaterial superlens. *Applied Physics Letters*, *90*(25), 254102. https://doi.org/10.1063/1.2750393

Berman, P. R. (2002). Goos-Hänchen shift in negatively refractive media. *Physical Review E, 66*, 067603. https://doi.org/10.1103/PhysRevE.66.067603

Boller, K. J., Imamoğlu, A., & Harris, S. E. (1991). Observation of electromagnetically induced transparency. *Physical Review Letters*, *66*, 2593. https://doi.org/10.1103/PhysRevLett.66.2593

Cubukcu, E., Aydin, K., Ozbay, E., Foteinopoulou, S., & Soukoulis, C. M. (2003). Negative refraction by photonic crystals. *Nature*, *423*, 604-605. https://doi.org/10.1038/423604b

Dong, M. H., Le, V. D., Vu, N. S., Dinh, X. K., & Nguyen, H. B. (2016). Propagation of a laser pulse in a three-level cascade atomic medium under conditions of electromagnetically induced transparency. *Photonics Letters of Poland*, *8*(3), 73-75. https://doi.org/10.4302/plp.2016.3.05

Dutta, S., & Dastidar, K. R. (2010). Realization of a negative refractive index in a three-level Λ system via spontaneously generated coherence. *Journal of Physics B: Atomic, Molecular and Optical Physics*, *43*(21), 215503. https://doi.org/10.1088/0953-4075/43/21/215503

Fang, A. P., Ge, W., Wang, M., Li, F., & Zubairy, M. S. (2016). Negative refraction without absorption via quantum coherence. *Physical Review A*, *93*(2), 023822. https://doi.org/10.1103/PhysRevA.93.023822

Jafarzadeh, H. (2017). All-optical switching in an open V-type atomic system. *Laser Physics*, *27*(2), 025204. https://doi.org/10.1088/1555-6611/27/2/025204

Krowne, C. M., & Shen, J. Q. (2009). Dressed–state mixed–parity transitions for realizing negative refractive index. *Physical Review A*, *79*(2), 023818. https://doi.org/10.1103/PhysRevA.79.023818

Le, V. D., & Dinh, X. K. (2021). Analyzing enhancement and control of Kerr-nonlinear coefficient in a three-level V-type inhomogeneously broadened atomic medium. *Dalat University Journal of Science*, *11*(1), 44-55. https://doi.org/10.37569/DalatUniversity.11.1.771(2021)

Le, V. D., & Vo, B. T. (2020). Light amplification based on electromagnetically induced transparency in a three-level V-type atomic system. *Dalat University Journal of Science*, *10*(3), 124-137. https://doi.org/10.37569/DalatUniversity.10.3.687(2020)

Liu, C., Zhang, J., Liu, J., & Jin, G. (2009). The electromagnetically induced negative refractive index in the Er^{3+}:$YAlO_3$ crystal. *Journal of Physics B: Atomic, Molecular and Optical Physics*, *42*(9), 095402. https://doi.org/10.1088/0953-4075/42/9/095402

McGloin, D., Fulton, D. J., & Dunn, M. H. (2001). Electromagnetically induced transparency in N-level cascade schemes. *Optics Communications*, *190*(1-6), 221-229. https://doi.org/10.1016/S0030-4018(01)01053-7

Nguyen, H. B., Le, V. D., & Dinh, X. K. (2019). Controllable optical properties of multiple electromagnetically induced transparency in gaseous atomic media. *Communications in Physics*, *29*(1), 1-33. https://doi.org/10.15625/0868-3166/29/1/13185

Nguyen, H. B., Nguyen, V. P., Vu, N. S., Nguyen, T. C., & Le, V. D. (2021). Negative refractive index in an inhomogeneously broadened four-level inverted-Y atomic medium. *IEEE Photonics Journal*, *13*(6), 2200407.https://doi.org/10.1109/JPHOT.2021.3119985

Nguyễn, T. A., Lâm, T. H., Tạ, T. A., & Lê, V. D. (2017). Điều khiển vận tốc nhóm ánh sáng dựa trên hiệu ứng trong suốt cảm ứng điện từ trong môi trường nguyên tử ^{87}Rb ba mức. *Tạp chí khoa học Trường Đại học Vinh*, *46*(2A), 21-30.

Nguyen, V. A., Nguyen, H. B., & Le, V. D. (2022). Negative refractive index in a Doppler broadened three-level Λ-type atomic medium. *Physica Scripta*, *97*(2), 025503. https://doi.org/10.1088/1402-4896/ac437a

Oktel, M. Ö., & Müstecaplıoğlu, Ö. E. (2004). Electromagnetically induced left-handedness in a dense gas of three-level atoms. *Physical Review A*, *70*(5), 053806. https://doi.org/10.1103/PhysRevA.70.053806

Othman, A. A., & Yevick, D. (2016). Enhanced negative refractive index control in a 5-level system. *Journal of Modern Optics*, *64*(12), 1208-1214. https://doi.org/10.1080/09500340.2016.1271914

Pendry, J. B. (2000). Negative refraction makes a perfect lens. *Physical Review Letters*, *85*(18), 3966-3969. https://doi.org/10.1103/PhysRevLett.85.3966

Pendry, J. B. (2003). Positively negative. *Nature*, *423*, 22-23. https://doi.org/10.1038/423022a

Phan, V. T., Ta, T. A., Le, C. T., Nguyen, T. D., Luong, T. Y. N., Dinh, X. K., Le, V. D., Nguyen, H. B., & Nguyen, V. A. (2016). Controlling optical bistability in a five-level cascade EIT medium. *Communications in Physics*, *26*(1), 33-42. https://doi.org/10.15625/0868-3166/26/1/8213

Sardar, D., Roy, S., Remesh, G., Gupta, S. D., & Deb, B. (2021). Realizing negative index of refraction in an ensemble of ground-state polar molecules with lasers. *Optics Communications*, *485*, 126742. https://doi.org/10.1016/j.optcom.2020.126742

Shen, J., Ruan, Z., & He, S. (2004). How to realize a negative refractive index material at the atomic level in an optical frequency range? *Journal of Zhejiang University-Science A*, *5*, 1322-1326. https://doi.org/10.1631/jzus.2004.1322

Steck, D. A. (2019). *Rubidium 85 D Line Data*. http://steck.us/alkalidata.

Veselago, V. G. (1968). The electrodynamics of substances with simultaneously negative values of ε and μ. *Soviet Physics Uspekhi*, *10*(4), 509-514. https://doi.org/10.1070/PU1968v010n04ABEH003699

Williams, J. M. (2001). Some problems with negative refraction. *Physical Review Letters*, *87*(24), 249703. https://doi.org/10.1103/PhysRevLett.87.249703

Yannopapas, V. (2006). Negative index of refraction in artificial chiral materials. *Journal of Physics: Condensed Matter*, *18*(29), 6883. https://doi.org/10.1088/0953-8984/18/29/025

Zhang, H., Niu, Y., & Gong, S. (2007). Electromagnetically induced negative refractive index in a V-type four-level atomic system. *Physics Letters A*, *363*(5-6), 497-501. https://doi.org/10.1016/j.physleta.2006.10.101

Zhang, H., Niu, Y., Sun, H., Luo, J., & Gong, S. (2008). Phase control of switching from positive to negative index material in a four-level atomic system. *Journal of Physics B: Atomic, Molecular and Optical Physics*, *41*(12), 125503. https://doi.org/10.1088/0953-4075/41/12/125503

Zhao, S.-C., Liu, Z.-D., & Wu, Q.-X. (2010). Left-handedness without absorption in the four-level Y-type atomic medium. *Chinese Physics B*, *19*(1), 014211. https://doi.org/10.1088/1674-1056/19/1/014211

Zhao, S.-C., Wu, Q.-X., & Gong, A.-L. (2013). Algebraic analysis of electromagnetic chirality-induced negative refractive index in a four-level atomic system. *The European Physical Journal D*, *67*(2), 28. https://doi.org/10.1140/epjd/e2012-30512-7